CrossMark
click for updates

Extreme ultraviolet induced defects on few-layer graphene

A. Gao,[1,a)] P. J. Rizo,[2] E. Zoethout,[1] L. Scaccabarozzi,[2] C. J. Lee,[1] V. Banine,[2] and F. Bijkerk[1,3]

[1]*FOM-Dutch Institute for Fundamental Energy Research, Edisonbaan 14, 3439 MN Nieuwegein, The Netherlands*
[2]*ASML, De Run 6501, 5504DR Veldhoven, The Netherlands*
[3]*MESA+ Institute for Nanotechnology, University of Twente, P.O. Box 217, 7500 AE Enschede, The Netherlands*

We use Raman spectroscopy to show that exposing few-layer graphene to extreme ultraviolet (EUV, 13.5 nm) radiation, i.e., relatively low photon energy, results in an increasing density of defects. Furthermore, exposure to EUV radiation in a H_2 background increases the graphene dosage sensitivity, due to reactions caused by the EUV induced hydrogen plasma. X-ray photoelectron spectroscopy results show that the sp^2 bonded carbon fraction decreases while the sp^3 bonded carbon and oxide fraction increases with exposure dose. Our experimental results confirm that even in reducing environment oxidation is still one of the main source of inducing defects. © 2013 AIP Publishing LLC. [http://dx.doi.org/10.1063/1.4817082]

I. INTRODUCTION

Graphene is a single planar sheet of sp^2 bonded carbon atoms which are closely packed in a honeycomb-like crystal structure. It is the basis of many carbon-based materials, e.g., stacked into graphite, rolled into carbon nanotubes, or wrapped into buckyballs.[1–3] Graphene has unique physical properties, such as quantum electronic transport, a tunable band gap, extremely high mobility, high elasticity, and electromechanical modulation.[3–8] This makes graphene a promising material for many applications, including graphene transistors, electronic circuits, and solar cells, as well as other applications in biology and chemistry.[3–8] However, one of the key requirements for such applications is the control of defects, such as vacancies, dislocations, or adatoms. The electronic properties of graphene are greatly affected by the presence of defects because they can act as scattering centers for electrons, reducing sheet conductivity.[9] Defects associated with dangling bonds can enhance the chemical reactivity of graphene.[10,11] Likewise, the presence of defects reduces the thermal conductivity of graphene.[12]

The unique properties make graphene an attractive candidate for applications in radiation-rich environment. However, the presence of defect may affect its performance. Therefore, it is critical to understand the radiation-induced damage in graphene. Zhou et al.,[13] reported that soft x-rays can easily break the sp^2 bond structure and form defects in graphene that is weakly bound to the substrate. Hicks et al.[14] also studied multilayer graphene, grown on SiC, before and after 10 keV x-ray irradiation in air. They concluded that defects were generated due to surface etching by reactive oxygen species created by x-rays. In this paper, we focus on defect generation in graphene, induced by exposure to 13.5 nm extreme ultraviolet (EUV) radiation under a variety of background conditions. We compare the rate at which defects are induced by EUV in a vacuum condition, and the rate at which defects are induced by exposure to EUV in a background of molecular hydrogen. We show that defects are introduced in both cases, though at different rates. Surprisingly, our data also show that, even in a reducing environment, oxidation is still one of the main sources of EUV induced defects. The experimental results are important for illustrating the damage-creating mechanisms upon photon interaction as well as designing graphene-based components for EUV lithography systems.

II. EXPERIMENTS

Graphene samples in this report were produced by the Graphene Supermarket. A few layers of graphene were grown on 25×25 mm^2 Ni/Si substrate with chemical vapor deposition method. The number of layers of graphene varies from 1 to 7, with an average of 4 over the sample. Three groups of experiments were performed: (1) a pristine sample served as a reference (refer to S_{ref}) and was not exposed; (2) a sample was exposed to EUV irradiation (S_{EUV}) without molecular hydrogen in the background gas; (3) a sample was exposed to EUV irradiation in a 5×10^{-2} mbar H_2 background (S_{EUV+H_2}). The other experimental settings are summarized in Table I. Graphene samples were irradiated by an EUV source (Philips EUV Alpha Source 2) with a repetition rate of 1 kHz and an average dose of 0.1 mJ/cm^2 per pulse. Raman spectra were collected with a home-built system. In this system, a 532 nm diode-pumped solid state laser is used to excite the samples

TABLE I. Experimental settings summary. Two parameters vary among different experiments: Exposure time to EUV radiation and/or H_2, hydrogen pressure.

Sample	S_{ref}	S_{EUV}	S_{EUV+H_2}
Exposure time (h)	NA	8	8
H_2 pressure (mbar)	NA	0	5×10^{-2}
Chamber pressure (mbar)	NA	1×10^{-8}	1×10^{-8}

a)Electronic mail: a.gao@differ.nl.

with an illumination spot of $3.5 \times 0.1 \, mm^2$ and a power density of $200 \, W/cm^2$. The collection efficiency of the detector system was calibrated using the HG-1 Mercury Argon Calibration Light Source and AvaLight-D(H)-S Deuterium-Halogen Light Source. 2D Raman intensity maps were acquired by collecting Raman signal over the central 2×0.1 mm^2 area. The transverse distance between two data points was set to $500 \, \mu m$, and along the longitudinal direction, the data points were collected continuously. X-ray photoelectron spectroscopy (XPS) was measured by monochromatic Al-Kalpha, Thermo Fisher Theta probe with a footprint of 1 mm diameter.

III. RESULTS AND DISCUSSION

A. Raman analysis

A typical Raman spectrum of graphene has three prominent features, i.e., D, G, and 2D peaks, located at $1350 \, cm^{-1}$, $1580 \, cm^{-1}$, and $2700 \, cm^{-1}$, respectively. The G peak is a first order Raman scattering process, corresponding to an in plane streching of sp^2 bonds. The D band is due to the breathing modes of six-atom rings, and requires a defect for activation. The 2D peak is the second order of the D peak. Since the 2D originates from a process where momentum conservation is satisfied by two phonons with opposite wavevectors, defects are not required for their activation, and are, thus, always present.[15,16] Fig. 1 shows the Raman spectra of the three samples. There is a small D peak in the spectrum of pristine sample, which is caused by natural defects such as edges, grain boundaries, or vacancies in graphene produced by CVD.[17,18] The spectrum for the sample that was exposed to EUV irradiation shows slightly higher D peak intensities compared to the pristine sample. The energetic photons from EUV irradiation might be expected to break sp^2 carbon bonds, leading to defects in graphene as well. The spectrum for the sample exposed to EUV in a hydrogen background has the highest D peak intensity. Besides the direct impact

from EUV photons, hydrogen is photo-ionized by the EUV radiation, resulting in atomic and molecular hydrogen ions, atomic hydrogen, and electrons.[19,20] Energetic electrons are known to break carbon bonds forming defects in graphene.[21,22] Furthermore, graphene hydrogenation occurs due to presence of a hydrogen plasma.[23] These combined effects lead to a higher defect density on the sample exposed to EUV in a hydrogen background. There is also a G peak shift from $1583 \, cm^{-1}$ for pristine sample to $1598 \, cm^{-1}$ for both S_{EUV} and S_{EUV+H_2}, indicating the formation of sp^2 clusters or chains.[24,25] Furthermore, there is another possible source for defects generation: secondary electrons from the Ni substrate, produced during EUV radiation. These electrons can be expected to have an energy less than 50 eV with a peak distribution between 2 and 5 eV.[26] These low energy electrons are not expected to create vacancy type defects. However, low energy electrons (7 eV) have been reported to dissociate adsorbed water and initiate oxide formation on metal surfaces.[27] This remains to be investigated.

Besides the single spectrum comparison, 2D scans for the two samples S_{EUV} and S_{EUV+H_2} were made to map the ratio of the D and G integrated intensities (shown in Fig. 2). In Fig. 2, the two samples S_{EUV} and S_{EUV+H_2} were partially covered with a metal mask. The spatial intensity distribution of EUV light is indicated in Figs. 2(a) and 2(d). Fig. 2(c) shows that S_{EUV+H_2} has a higher D/G value, within exposed area, than that for S_{EUV}. It is also noted that for D/G ratio maps of the samples S_{EUV} and S_{EUV+H_2}, there is a clear distinction between the exposed and unexposed areas. The D/G ratio map in Fig. 2(a) clearly coincides with the EUV intensity profile shown in Fig. 2(b). The D/G ratio is also plotted as a function of EUV dose for both S_{EUV} and S_{EUV+H_2} samples in Figs. 3(a) and 3(b). The D/G ratio first grows as the EUV intensity increases, then saturates. It appears that for S_{EUV} the D/G ratio does not saturate as the EUV dose increases. Note that the I(D)/I(G) of S_{EUV} value is lower than the ratio of S_{EUV+H_2}, indicating that it may saturate at higher values.

B. XPS analysis

Quantitative information on the relative concentrations of different C bond types in the sample was obtained by analyzing the C1s peak of the XPS spectrum.[28,29] The curve fitting results for the C1s spectrum of S_{EUV+H_2} are shown in Fig. 4(a). There are four components in the C1s spectrum: the first peak at binding energy 283.4 eV, which is attributed to carbide formation with the underlying Ni layer, the second peak, at binding energy 284.4 eV, corresponds to the sp^2 bonds in graphitic like carbon, the third peak, at binding energy 285.3 eV, corresponds to carbon bonds with sp^3 hybridization, and the fourth peak, at binding energy 286.8 eV, is assigned to hydroxyl group. The appearance of sp^3 carbon and C-OH both indicate the generation of defects in graphene. Oxidation occurs when graphene reacts with the residual water during exposure. At the same time, oxidation will generate at least one sp^3 bond as well. The sp^3 bonds can also be introduced by hydrogen plasma generated under EUV irradiation. In Fig. 4(b), for both the S_{EUV+H_2} and S_{EUV}
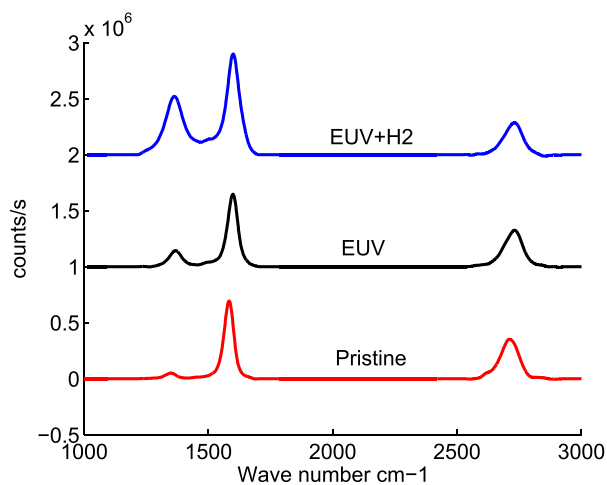
FIG. 1. Comparison of the Raman spectra and the spectrum for the example exposed to EUV in a hydrogen background has the highest D peak intensity. The spectra for the samples exposed to EUV irradiation show slightly lower D peak intensity. The pristine sample has the lowest D peak intensity. Note that the spectra are separated by an offset of 5×10^5 counts/s.

(a) EUV Intensity profile   (b) EUV only   (c) EUV+H₂   (d) EUV Intensity profile
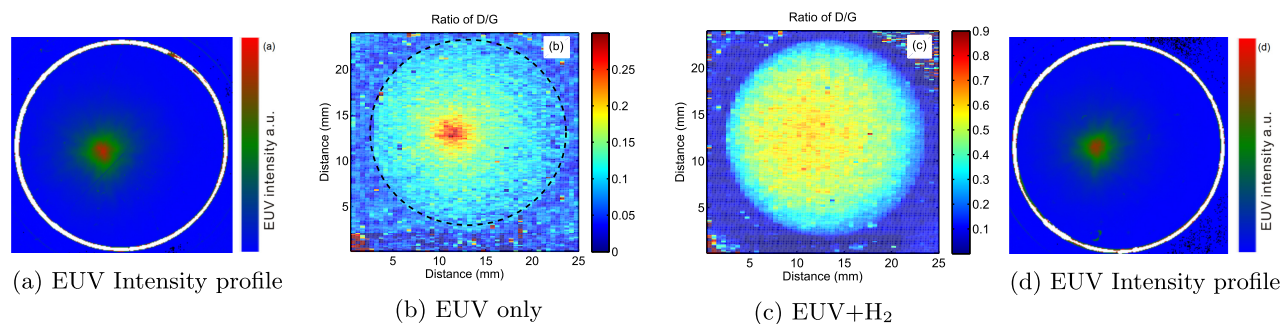
FIG. 2. $I(D)/I(G)$ ratio mapping. (b) and (c) are $I(D)/I(G)$ ratio maps for S_{EUV} and S_{EUV+H_2}. (a) and (d) are the EUV intensity profiles for S_{EUV} and S_{EUV+H_2}, respectively. The white circle indicates the mask boundary.
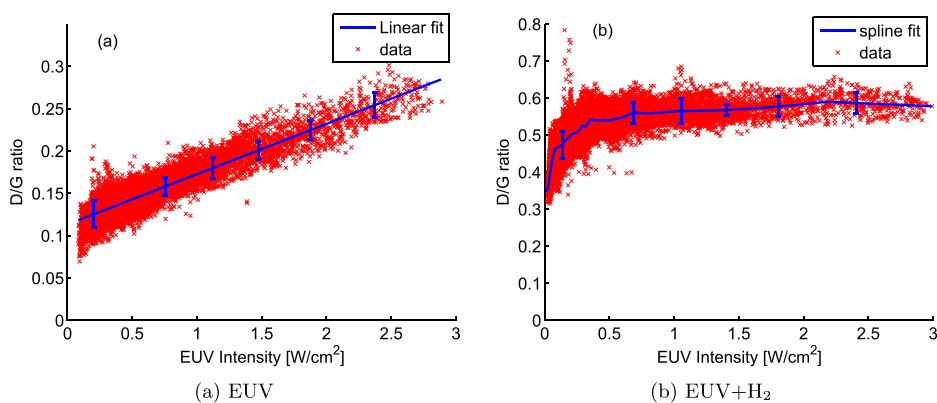

(a) EUV   (b) EUV+H₂

FIG. 3. $I(D)/I(G)$ ratio versus EUV power.
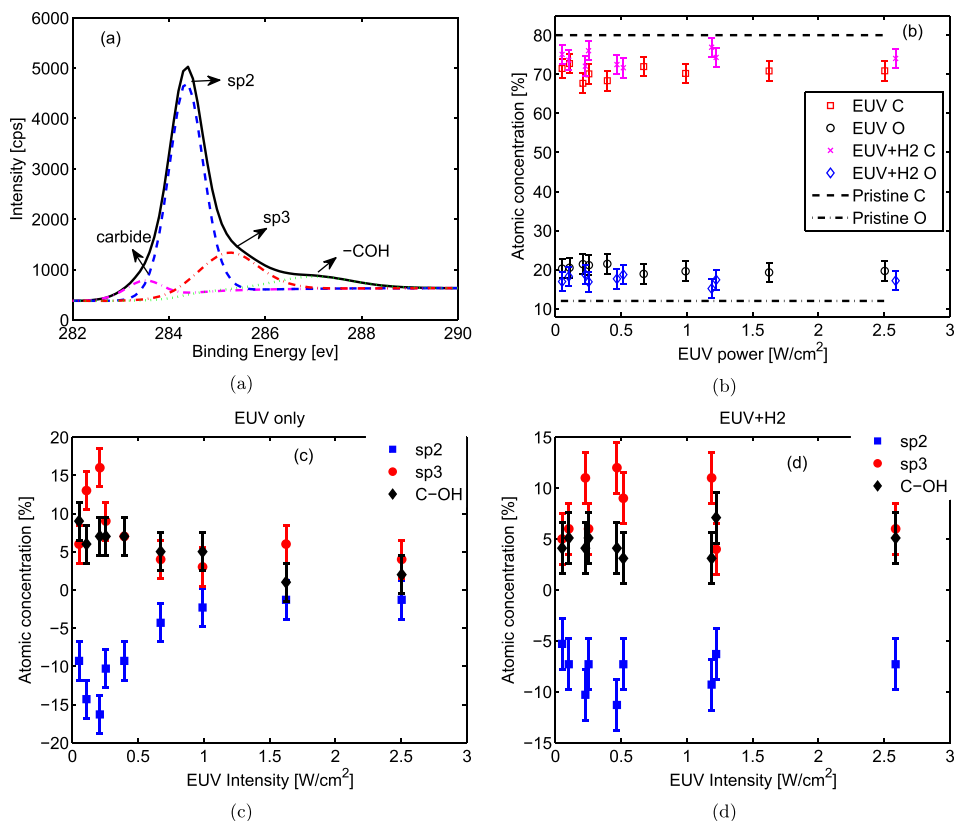

(a)   (b)   (c)   (d)

FIG. 4. (a) XPS analysis: curve fitting results for S_{EUV}; (b) Element concentration versus EUV power for S_{EUV+H_2} and S_{EUV}; (c) and (d) Bond concentration change with respect to the pristine sample versus EUV power for S_{EUV} and S_{EUV+H_2}.

sample, we can see that C element (the sp^2 bonded carbon) concentration drops by 5%–9% and O element concentration increases by 5%–8% compared with that in pristine sample. The concentration change of different bonds versus EUV power with respect to the pristine sample are plotted in Figs. 4(c) and 4(d). In the case of S_{EUV}, the sp^2 concentration decreases less in the higher power range than in the lower power ranges. It appears that under EUV irradiation, besides breaking sp^2 bonds and forming sp^3 and C-OH bonds, there is also a transformation from C-OH phase to sp^2 phase, since the C-OH concentration change drops to almost zero. This transformation can be induced by local heating[30] due to EUV irradiation. However, this transformation does not indicate that the converted sp^2 bonds are forming an ordered ring structure like in the undistorted graphene network, since, in the Raman spectrum, I(D)/I(G) (Fig. 3(a)) increases in higher EUV power range. In contrast, for S_{EUV+H_2}, the transformation to sp^2 is neglectable. Because hydrogenation can be the dominant effect, the converted sp^2 bonds will be hydrogenated in the end. Besides forming C-OH (oxidation), forming C-H bond (hydrogenation) will generate C-C (sp^3) bonds as well. The sp^3 concentration increases slowly at low intensities (lower than 0.5 W/cm^2) and saturates at higher powers, which coincide with the I(D)/I(G) ratio map in Fig. 3(b). However, comparing S_{EUV+H_2} with S_{EUV}, even with the same amount of sp^2, sp^3, and C-OH, they show different I(D)/I(G) values, indicating that there is no unique quantitative relationship between I(D)/I(G) ratio and sp^3 or C-OH content. The contribution from C-H or C-OH solely to I(D)/I(G) has yet to be investigated. Nevertheless, the XPS data clearly show that the defects were generated by EUV photons, including hydrogenation, and oxidation even in a reducing environment (H$_2$).

IV. CONCLUSION

The Raman results reported here show that there are defects induced in graphene after EUV irradiation, which is reflected by an increase of the D peak intensity. The defects are caused by breaking sp^2 bonds by EUV photons, oxidation due to the formation of OH groups, hydrogenation due to hydrogen plasma generated during EUV irradiation. The XPS results confirm that, after EUV irradiation, the concentration of sp^2 bonds in graphene decreases while the concentration of sp^3 bonds and C-OH bonds increases, clearly indicating defects generated in graphene. EUV irradiation introduces defects both through oxidation with the residual water background, and more effectively by hydrogenation due to the presence of hydrogen plasma.

ACKNOWLEDGMENTS

[1]A. Geim and K. Novoselov, "The rise of graphene," Nature Mater. **6**, 183–191 (2007).

[2]A. Geim, "Graphene: Status and prospects," Science **324**, 1530–1534 (2009).

[3]K. Novoselov, D. Jiang, F. Schedin, T. Booth, V. Khotkevich, S. Morozov, and A. Geim, "Two-dimensional atomic crystals," Proc. Natl. Acad. Sci. U.S.A. **102**, 10451 (2005).

[4]Y. Zhang, Y. Tan, H. Stormer, and P. Kim, "Experimental observation of the quantum hall effect and berry's phase in graphene," Nature **438**, 201–204 (2005).

[5]M. Han, B. Özyilmaz, Y. Zhang, and P. Kim, "Energy band-gap engineering of graphene nanoribbons," Phys. Rev. Lett. **98**, 206805 (2007).

[6]K. Bolotin, K. Sikes, Z. Jiang, M. Klima, G. Fudenberg, J. Hone, P. Kim, and H. Stormer, "Ultrahigh electron mobility in suspended graphene," Solid State Commun. **146**, 351–355 (2008).

[7]C. Lee, X. Wei, J. Kysar, and J. Hone, "Measurement of the elastic properties and intrinsic strength of monolayer graphene," Science **321**, 385–388 (2008).

[8]J. Bunch, A. Van der Zande, S. Verbridge, I. Frank, D. Tanenbaum, J. Parpia, H. Craighead, and P. McEuen, "Electromechanical resonators from graphene sheets," Science **315**, 490–493 (2007).

[9]D. Boukhvalov and M. Katsnelson, "Chemical functionalization of graphene with defects," Nano Lett. **8**, 4373–4379 (2008).

[10]A. Cortijo and M. Vozmediano, "Effects of topological defects and local curvature on the electronic properties of planar graphene," Nucl. Phys. B **763**, 293–308 (2007).

[11]G. Rutter, J. Crain, N. Guisinger, T. Li, P. First, and J. Stroscio, "Scattering and interference in epitaxial graphene," Science **317**, 219–222 (2007).

[12]F. Hao, D. Fang, and Z. Xu, "Mechanical and thermal transport properties of graphene with defects," Appl. Phys. Lett. **99**, 041901 (2011).

[13]S. Zhou, Ç. Girit, A. Scholl, C. Jozwiak, D. Siegel, P. Yu, J. Robinson, F. Wang, A. Zettl, and A. Lanzara, "Instability of two-dimensional graphene: Breaking sp^2 bonds with soft x rays," Phys. Rev. B **80**, 121409 (2009).

[14]J. Hicks, R. Arora, E. Kenyon, P. Chakraborty, H. Tinkey, J. Hankinson, C. Berger, W. de Heer, E. Conrad, and J. Cressler, "X-ray radiation effects in multilayer epitaxial graphene," Appl. Phys. Lett. **99**, 232102 (2011).

[15]A. Ferrari, J. Meyer, V. Scardaci, C. Casiraghi, M. Lazzeri, F. Mauri, S. Piscanec, D. Jiang, K. Novoselov, and S. Roth, "Raman spectrum of graphene and graphene layers," Phys. Rev. Lett. **97**, 187401 (2006).

[16]A. Ferrari, "Raman spectroscopy of graphene and graphite: Disorder, electron–phonon coupling, doping and nonadiabatic effects," Solid State Commun. **143**, 47–57 (2007).

[17]A. Eckmann, A. Felten, A. Mishchenko, L. Britnell, R. Krupke, K. Novoselov, and C. Casiraghi, "Probing the nature of defects in graphene by Raman spectroscopy," Nano Lett. **12**(8), 3925–3930 (2012).

[18]M. Gass, U. Bangert, A. Bleloch, P. Wang, R. Nair, and A. Geim, "Free-standing graphene at atomic resolution," Nat. Nanotechnol. **3**, 676–681 (2008).

[19]Y. Chung, E. Lee, T. Masuoka, and J. Samson, "Dissociative photoionization of h from 18 to 124 ev," J. Chem. Phys. **99**, 885 (1993).

[20]H. Kossmann, O. Schwarzkopf, B. Kämmerling, and V. Schmidt, "Unexpected behaviour of double photoionization in h_{2}," Phys. Rev. Lett. **63**, 2040–2043 (1989).

[21]D. Teweldebrhan and A. Balandin, "Modification of graphene properties due to electron-beam irradiation," Appl. Phys. Lett. **94**, 013101 (2009).

[22]M. Iqbal, A. Kumar Singh, M. Iqbal, S. Seo, and J. Eom, "Effect of e-beam irradiation on graphene layer grown by chemical vapor deposition," J. Appl. Phys. **111**, 084307 (2012).

[23]D. Elias, R. Nair, T. Mohiuddin, S. Morozov, P. Blake, M. Halsall, A. Ferrari, D. Boukhvalov, M. Katsnelson, and A. Geim, "Control of graphene's properties by reversible hydrogenation: Evidence for graphene," Science **323**, 610–613 (2009).

[24]A. Ferrari and J. Robertson, "Interpretation of Raman spectra of disordered and amorphous carbon," Phys. Rev. B **61**, 14095 (2000).

[25]K. N. Kudin, B. Ozbas, H. C. Schniepp, R. K. Prud'Homme, I. A. Aksay, and R. Car, "Raman spectra of graphite oxide and functionalized graphene sheets," Nano Lett. **8**, 36–41 (2008).

[26]J. Scholtz, D. Dijkkamp, and R. Schmitz, "Secondary electron emission properties," Philips J. Res. **50**, 375–389 (1996).

[27]H. Ebinger and J. Yates, "Electron-impact-induced oxidation of al (111) in water vapor: Relation to the cabrera-mott mechanism," Phys. Rev. B **57**, 1976 (1998).

[28]S. Kaciulis, "Spectroscopy of carbon: From diamond to nitride films," Surf. Interface Anal. **44**(8), 1155–1161 (2011).

[29]P. Patsalas, M. Handrea, S. Logothetidis, M. Gioti, S. Kennou, and W. Kautek, "A complementary study of bonding and electronic structure of amorphous carbon films by electron spectroscopy and optical techniques," Diamond Relat. Mater. **10**, 960–964 (2001).

[30]A. Bagri, C. Mattevi, M. Acik, Y. Chabal, M. Chhowalla, and V. Shenoy, "Structural evolution during the reduction of chemically derived graphene oxide," Nat. Chem. **2**, 581–587 (2010).